III making some contribution. The electron distribution featured in I is in accord with the concept of a cycloaddition or insertion of the PhC≡CPh molecule into the $Ru_2(Htmtaa)(O_2CCH_3)_3$ moiety. As a result, the diphenylacetylene group becomes a bridge between the methine carbon atom, C(2), of the tmtaa ligand and the two ruthenium atoms. This has much in common with an earlier report[12] of the addition of acetylene across the 2,4-pentanediiminato chelate ring and a cobalt atom in a mononuclear Co–tmtaa complex.

Concluding Remarks

In summary, the synthesis and characterization of the unprecedented title compound adds yet another example to the wide range of fascinating transition-metal complexes containing the dibenzo[*b*,*i*]-1,4,8,11 tetraazacyclotetradecine macrocyclic ligand. It can be concluded that the unique features of tmtaa, as listed in the Introduction, are the ones responsible for the continuing discoveries of a variety of new compounds.

In our ruthenium dimer, the macrocycle becomes a tridentate, uninegatively charged ligand, which for the first time uses one of its four nitrogen atoms to bridge two metal centers. In addition, the ruthenium dimer is a novel compound from the bonding point of view. It exhibits four η^2-type interactions between the Ru_2 core and the surrounding ligands as well as a metal–carbon bond that has the negative charge localized on the carbon.

The straightforward reaction of $Ru_2(O_2CCH_3)_4$, H_2tmtaa, and PhCCPh leads to a complex that, together with one one other example of a metal–metal bonded dimer containing one tmtaa ligand,[13] may lead the way to a new class of such compounds. Chemistry of this kind is currently under investigation.

Acknowledgment. We thank the National Science Foundation for their support.

Supplementary Material Available: Tables containing full listings of bond distances, bond angles, anisotropic displacement parameters (*B*'s), and positional and equivalent isotropic thermal parameters for $Ru_2(Htmtaa)(O_2CCH_3)_3(PhCCPh)$ (15 pages); table of observed and calculated structure factors (33 pages). Ordering information is given on any current masthead page.

(12) Weiss, M. C.; Gordon, G. C.; Goedken, V. L. *J. Am. Chem. Soc.* **1979**, *101*, 857.

(13) Guerchais, J., private communication on the $Mo_2(O_2CCH_3)_2(tmtaa)$ complex.

Regulation of Molecular Conformation of Chiral Tripodal Structures by Ca^{2+} Binding

Izac Dayan,[†] Jacqueline Libman,[†] Abraham Shanzer,*[,†] Clifford E. Felder,[‡] and Shneior Lifson*[,‡]

Contribution from the Department of Organic Chemistry and Department of Chemical Physics, The Weizmann Institute of Science, Rehovot 76100, Israel. *Received January 22, 1990. Revised Manuscript Received December 5, 1990*

Abstract: Chiral ligands are introduced whose conformations may be regulated by the presence of Ca^{2+} ions. These compounds are assembled from two types of C_3-symmetric molecules as anchors (type I and type 2) and extended by chiral peptide residues. Their ion-binding properties are examined by a combination of experimental and theoretical tools (empirical force field (EFF) calculations). The calculations provide a conceptual framework in which to relate all the experimental observations into a coherent picture. The first type of compounds is shown to form complexes of prismatic geometry, inherently unfit to generate chiral complexes, while the second type forms complexes of octahedral coordination. Some of the ligands are found to generate Ca^{2+} complexes of optically active configurations and to thereby represent the first examples of chiral alkaline earth metal complexes. Ca^{2+} ions may thereby provide a viable exogenous means for the generation of chiral receptors from randomly arranged tripod-like molcules.

Introduction

Recently, we have introduced C_3-symmetric trispeptides that adopt propeller-like conformations of defined chiral sense by virtue of a belt of interstrand (or circular) H-bonds.[1] Extension of these trispeptides by ion binding groups such as catecholates[2] or hydroxamates[3], provided chiral receptors specific for ferric ions that mimic the properties of natural siderophores.[2,3] The absolute configuration of the resulting ferric complexes was found to be imposed by the chiral network of H-bonds in the receptor molecule.

However, the generation of chiral receptors from tripod-like molecules by H-bonds is generally limited to nonpolar solutions. In order to create chiral receptors also in polar media where H-bonds are broken, we aimed at generating tripod-like molecules whose conformation could be shaped by binding to alkali and alkaline earth metal ions as organizing elements. Such ion-induced intramolecular organization was envisioned to have the additional advantage of allowing exogenous control and regulation. Alkali and alkaline earth metal ions were conceived as eminently suitable for this task as they are characterized by fast-exchange kinetics. Among this family of metal ions, Ca^{2+} ions appeared to be particularly promising because of their high plasticity to fit various coordination geometries.[4,5] Extending such chiral ligands with binding cavities for ferric ions, for example, was anticipated to provide regulateable ferric ion carriers.

In this paper, we introduce tripod-like ligands (Figure 1) that form Ca^{2+} complexes of high chiral preference and thereby

[†] Department of Organic Chemistry.
[‡] Department of Chemical Physics.

(1) Tor, Y.; Libman, J.; Shanzer, A.; Felder, C. E.; Lifson, S. *J. Chem. Soc., Chem. Commun.* **1987**, 749.
(2) Tor, Y.; Libman, J.; Shanzer, A.; Lifson, S. *J. Am. Chem. Soc.* **1987**, *109*, 6517.
(3) Tor, Y.; Libman, J.; Shanzer, A. *J. Am. Chem. Soc.* **1987**, *109*, 6518.
(4) Williams, R. J. P. Calcium-Binding Proteins Health Disccussion (International Symposium); Norman, A. W. Vanaman, T. C., Means, A. R., Eds.; Academic Press: New York, 1987; 149. Williams, R. J. P. Ciba Found. Symp. **1986**, *122* (Calcium Cell), 145.
(5) Neupert-Laves, K.; Dobler, M. *Helv. Chim. Acta* **1977**, *60*, 1861.

0002-7863/91/1513-3431$02.50/0

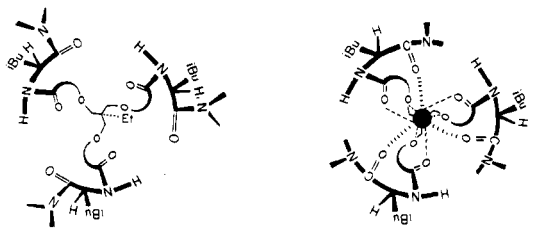

Figure 1. Schematic representation of Ca^{2+}-binding ligands: left, free ligand; right, Ca^{2+} complex.

demonstrate that the creation of chiral receptors by exogenous means is a viable possibility. We combine experimental with theoretical tools to elucidate the relationship between the nature of the ligating groups and the geometry of the resulting Ca^{2+} complexes. In this combined experimental–theoretical approach, calculations provide a conceptual framework in which to relate the experimental facts into a single, coherent picture. To the extent that the calculations agree with experimental findings, the emerging conclusions reflect reality with considerable confidence. The advantages of the theoretical approach as well as its limitations are discussed in the Methods.

Two families, or types, of oxa–amide binders were synthesized and examined, of which only the second family proved to form chiral complexes with Ca^{2+} ions. The first family, type 1, resembles the metal-ion binders developed by Simon.[6] The second family, type 2, is a modification of type 1 by containing a two-methylene bridge rather than a one-methylene bridge between the ether group and the amide carbonyl. Each type has three members that differ in the end groups of the tripodal strands. The end groups are either (a) achiral chains (R = $-NHC_7H_{15}$), (b) chiral inert hydrocarbon residues (R = $-NHC^*HCH_3Ph$), or (c) chiral residues containing amide groups as additional ion-binding sites (R = $-NHC^*H$-*i*-BuCONEt$_2$).

$$EtC(CH_2O(CH_2)_nCOR)_3$$

1, $n = 1$
2, $n = 2$
a, R = $-NHC_7H_{15}$
b, R = $-NHC^*HCH_3Ph$
c, R = $-NHC^*H$-*i*-BuCONEt$_2$

The absolute configuration of C* in compounds b and c is *S*. The conformations and binding properties of these molecules and their Ca^{2+} complexes were examined by NMR, IR, and CD spectrometry and by theoretical calculations of the stable conformations of the Ca^{2+} complexes and their energies using the empirical force field method (EFF).

Methods

Experimental Methods. IR was utilized to determine the involvement of the amide carbonyl groups in binding by the occurrence of a red (bathochromic) shift of the C=O stretching frequency. A larger red shift for the same type of carbonyl group (whether secondary or tertiary amide) was interpreted as a stronger ion–oxygen bond. This rule stems from a more general, well-established rule that the longer the equilibrium length of a given bond the smaller its stretching force constant and the lower its IR frequency. The C=O bond is stretched when polarized by the Ca^{2+} ion, but other factors such as changes in the vicinal bond angles may also affect the bond length. To the best of our knowledge, no systematic study has so far been performed on the correlation between red shifts of carbonyl groups and oxygen–metal bond distances. Neither did we find any values for carbonyl shifts induced by calcium binding. Yet, the observed shifts (see Table I and Figure 2) are significant when compared with literature data for carbonyl binding to alkali metal ions. Binding of K^+ to valinomycin, for example, has been reported to induce a bathochromic shift of the ester carbonyls of -7.0 cm^{-1},[7] and binding of synthetic lactones to Na^+ was reported to cause a shift of -20 cm^{-1}.[8]

(6) Gueggi, M.; Oehme, M.; Pretsch, E.; Simon, W. *Helv. Chim. Acta* **1976**, *59*, 2417.
(7) Funck, Th.; Eggers, F.; Grell, E. *Chimia* **1972**, *26*, 637.
(8) Tajima, I.; Okada, M.; Sumitomo, H. *J. Am. Chem. Soc.* **1981**, *103*, 4096.

Table I. IR Frequencies (cm^{-1}) of Free Ligands and of Their Ca^{2+} Complexes

compd	solvent	C=O^{I} ligand	C=O^{I} complex	C=O^{I} shift	C=O^{II} ligand	C=O^{II} complex	C=O^{II} shift
1a	CD_3CN	1674	1657	−17			
	$CDCl_3$	1672					
1b	CD_3CN	1676	1654	−22			
	$CDCl_3$	1671	1655	−16			
1c	CD_3CN	1678	1645	−33	1640	1621	−19
	$CDCl_3$	1675	1659	−16	1636	1635	−1
2a	CD_3CN	1669	1641	−28			
	$CDCl_3$	1657					
2b	CD_3CN	1670	1639.5	−30.5			
	$CDCl_3$	1659	1629.0	−30.0			
2c	CD_3CN	1668	1633	−35	1641	1633	−8
	$CDCl_3$	1659	1631	−28	1634	1630	−4

Table II. NMR ^{1}H Shifts of Free Ligands (δ) and the Induced Chemical Shifts ($\Delta\delta$) of Their Ca^{2+} Complexes

		CCH_2O		OCH_2		CH_2CO	
compd	solvent	δ	$\Delta\delta^a$	δ	$\Delta\delta^a$	δ	$\Delta\delta^a$
1a	CD_3CN	3.43 (s)	0.26			3.84 (s)	0.33
	$CDCl_3$	3.4 (s)				3.96 (s)	
1b	CD_3CN	3.43 (s)	0.24			3.82 (s)	0.37
	$CDCl_3$						
1c	CD_3CN	3.49 (s)	0.20			3.93 (s)	0.32
	$CDCl_3$	3.51 (s)				4.05 (ABq)	
						3.99 (ABq)	
2a	CD_3CN	3.20 (s)	0.40	3.58 (t)	0.16	2.28 (t)	0.26
	$CDCl_3$	3.25 (s)		3.66 (m)		2.46 (m)	
2b	CD_3CN	3.08 (s)	0.40	3.51 (m)	−0.14	2.25 (m)	0.08
			0.29				0.23
2c	CD_3CN	3.18 (s)	0.51	3.59 (m)	0.26	2.33 (m)	0.15
			0.31		0.01	2.45 (m)	0.23
	$CDCl_3$	3.28 (s)		3.65 (t)		2.48 (m)	

[a] Two values for $\Delta\delta$ indicate the appearance of two signals for the diastereotopic protons after ion binding.

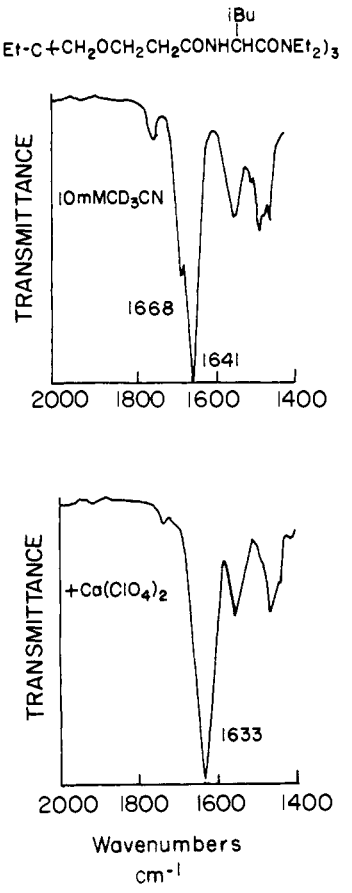

Figure 2. IR spectra of ligand **2c** and of its Ca^{2+} complex.

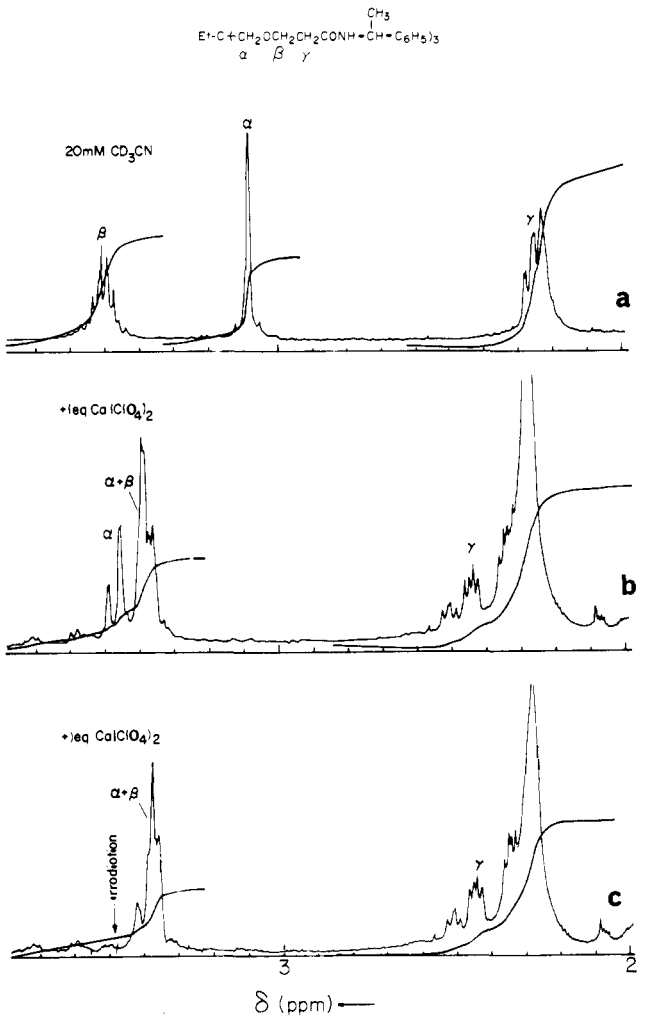

Figure 3. NMR trace of ligand **2b** (trace a) and of its Ca^{2+} complex (trace b), and the decoupled spectrum of the Ca^{2+} complex (trace c).

Table III. NMR ^{13}C Shifts of Free Ligands **1c** and **2c** and the Induced Chemical Shifts ($\Delta\delta$) of Their Ca^{2+} Complexes[a]

type of C	**1c** (δ)	**1c** + Ca^{2+} ($\Delta\delta$)	**2c** (δ)	**2c** + Ca^{2+} ($\Delta\delta$)
C=O[I]	169.654	+1.450	172.737	+2.376
C=O[II]	172.101	+0.222[b]	171.687	−0.007
$C(CH_2O)$	73.372	+5.725	71.424	+6.709
$-OCH_2-$	71.704	−0.101	68.297	+0.515
$CH_2C=O$			37.279	−3.739
CH-*i*-Bu	47.613	+1.463	47.934	+2.218

[a] The measurements were performed in 20 mM CD_3CN solution on a 500 MHz Bruker instrument. Chemical shifts are given relative to internal TMS. The assignments are based on off-resonance spectra of a series of related compounds. For the numbering of the carbon atoms, see Table IV and footnote. [b] The smallness of the induced shift is attributed to conformational changes that take place upon complexation and cause shielding of C=O[II].

Binding of DMF to Li^+ has been reported to cause a red shift of 16 cm^{-1}.[9]

^1H NMR titration of the ligands with calcium perchlorate was used to establish (i) the stoichiometry of binding, (ii) the location of the metal ion, and (iii) the possible formation of complexes with a preferred chiral sense by the appearance of distinctly different chemical shifts for each of the diastereotopic methylene protons. The ^1H NMR data are presented in Table II and for a specific case in Figure 3.

The free ligands **1c** and **2c** and their Ca^{2+} complexes were further examined by ^{13}C NMR. ^{13}C NMR was employed to supplement information gained from IR by providing a measure for the extent of change in the polarization of the C=O carbonyl carbon upon binding. The ^{13}C NMR data are presented in Table III.

(9) Lassigne, C.; Baine, P. *J. Phys. Chem.* **1971**, *30*, 3188.

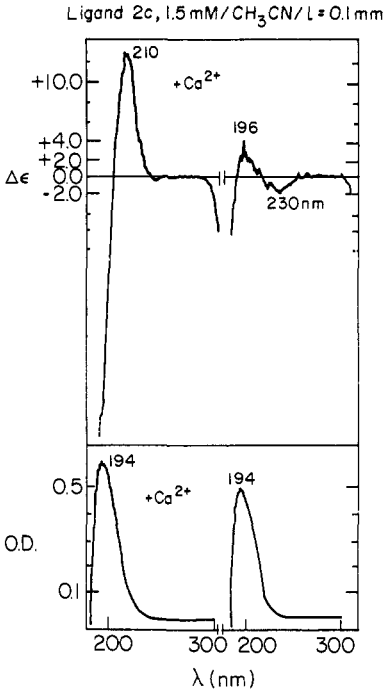

Figure 4. UV and CD Spectra of ligand **2c** and of its Ca^{2+} complex.

CD measurements of the free chiral ligands and their Ca^{2+} complexes were used to determine whether the metal complexes had a preferred chiral sense by the appearance of exciton coupling between the ion-binding carbonyl groups. Exciton coupling is anticipated to occur upon binding as a consequence of conformational constraint of the ligating groups. If one of the two possible diasteromeric complexes is preferred, exciton coupling manifests itself as enhanced negative or positive Cotton effects symmetrically displaced relative to the UV absorption. The CD spectra of representative examples are given in Figure 4.

We used acetonitrile as solvent for the titration experiments since acetonitrile readily solubilizes the free ligands, the Ca^{2+} salts, and the Ca^{2+} complexes and is fit for all spectroscopic analyses including IR, NMR, UV, and CD. However, one of the reviewers suggested that solvent molecules might be incorporated into the coordination sphere of the Ca^{2+} ion. In order to examine solvent effects, the IR spectra of ligands of both families, namely **1b**, **1c**, **2b**, and **2c**, and of their Ca^{2+} complexes were also tested in chloroform and compared with those in acetonitrile (Table I). We used chloroform, rather than carbon tetrachloride, since carbon tetrachloride hardly solubilizes even the free ligands, let alone the salts or the Ca^{2+} complexes.

Theoretical Methods. The EFF calculations of the Ca^{2+} ligand complexes supplemented the IR, NMR, and CD measurements with a wealth of conformational and energetic data. Correlating the calculated and the experimental data helped to interpret the results and provide a comprehensive overview of the properties of the complexes.

Calculated data of interest are presented in Table IV for all equilibrium conformations within the range of 5 kcal/mol above the minimum energy. Stereoviews of most of these conformations are also presented. The data in Table IV comprise (1) the equilibrium energy relative to the most stable state; (2) the distances of the Ca^{2+} ion to its binding oxygens; (3) the chirality of the complex; and (4) the torsional angles that represent the conformations of the complexes. While the energy was minimized for all internal coordinates, these torsional angles are sufficient for discussing and comparing the different conformations.

The EFF was used by us in the last few years to great advantage in the analysis of the properties of natural ion carriers and their ion complexes[10-15] as well as in designing new ion carriers and in predicting their

(10) Lifson, S. In *Supramolecular Structure and Function*; Pifat, G., Herak, J. N., Eds.; Plenum: New York and London, 1983; pp 1–44.
(11) Lifson, S.; Felder, C. E.; Shanzer, A.; Libman, J. In *Synthesis of Macrocycles: The Design of Selective Complexing Agents*; Izatt, R. M., Christensen, J. J., Eds.; 1987; pp 241–307.
(12) Lifson, S.; Felder, C. E.; Shanzer, A. *J. Am. Chem. Soc.* **1983**, *105*, 3866–3875.
(13) Lifson, S.; Felder, C. E.; Shanzer, A. *Biochemistry* **1984**, *23*, 2577–2590.
(14) Lifson, S.; Felder, C. E.; Shanzer, A. *J. Biomol. Struct. Dyn.* **1984**, *2*, 641–661.

Table IV. Calculated Ca^{2+} Complexes of Tripod Ligands

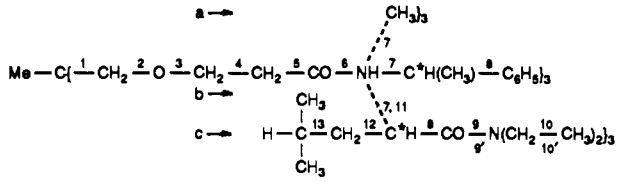

compd	ΔE_{tot}[a]	O···Ca[b]	CO···Ca[b] CO[I]	CO[II]	conf[c]	torsional angles[d] 1	2	3	4	5	6	7	8	9	10	9′	10′	11	12	13
1a	0.0	2.47	2.43		P	180	180	180		180	180									
2a	0.0	2.40	2.39		R	180	∓174	180	∓60	∓101	±177									
	2.2	2.41	2.39		R	±176	±175	∓103	∓69	∓137	∓179									
1b	0.0	2.48	2.42		P	178	−172	159		−131	163	−63	−60							
	0.1	2.50	2.42		P	177	179	173		−138	165	60	69							
2b	0.0	2.41	2.38		Λ	180	172	−178	61	112	179	56	56							
	0.6	2.40	2.39		Λ	−178	172	−174	54	83	−171	158	72							
	1.4	2.42	2.37		Δ	−179	−174	−177	−59	−101	177	51	71							
1c	0.0	2.94	2.56	2.50	ΔΛ	167	−111	164		103	−158	72	140	−172	−84	5	−94	−57	−58	56
		2.77	2.57	2.58		173	−154	165		117	−169	74	143	178	−106	−2	−88	−55	−59	57
		2.74	2.58	2.48		166	−119	177		101	−152	71	137	−177	−84	4	−92	−57	−59	56
	0.9	2.51	3.50	2.40	PΔ	174	−176	158		−76	154	−52	155	167	−93	−9	−86	−177	73	50
2c	0.0	2.64	2.55	2.70	ΔΛ	176	−161	94	68	95	−165	73	144	−172	105	3	149	−56	−56	58

[a] Total conformational energies (kcal/mol) relative to the energy-minimum state. [b] Calcium–oxygen binding distances (Å). [c] Chirality of the configuration about the bound calcium. P represents prismatic and R represents a racemic mixture of two enantiomers. In the case of nonacoordination (**1c** and **2c**), the double notation represents the first carbonyls relative to the ethers, followed by the second carbonyls relative to the first carbonyls. [d] Angles (deg) defined according to the following scheme for molecules a, b, and c, respectively: For **1c** and **2c**, torsions 1–8 are the backbone torsions, 9 and 10 refer to one end group and 9′ and 10′ to the second end group on each chain. Torsions 11–13 refer to the isopropyl side chains, with torsion 13 taken with respect to the tertiary H.

properties.[1,2,12] EFF calculations were so far successfully performed only on molecules and complexes in vacuum or on crystals, since calculations of molecules in solution are orders of magnitude more difficult and less reliable. Application to molecules in solution was, however, rendered meaningful in several ways.

First, solvent effects cancel out substantially when differences in binding strengths and conformations of the same ligand with different ions[13,14] or the same ion with related compounds[14,15] are calculated. Second, solution properties in solvents of different polarities can be extrapolated to vacuum, since vacuum approximates nonpolar solvents better than polar ones. For example, intramolecular hydrogen bonds that were predicted to exist in vacuum were not observed in methanol, partly observed in chloroform, and fully observed in carbon tetrachloride.[1] Third, in many cases intramolecular interactions predominate over intermolecular ones. This is particularly true for ion–ligand interactions.

Thus, EFF-calculated conformations of single ligand–ion complexes in vacuum agreed well with the crystallographic data whenever these were available.[11] On the other hand, when a flexible free ligand was distorted by crystal forces, EFF derived the distortion from the calculated equilibrium conformations of the same molecule in vacuum[13] and in crystals.[16] The EFF also helped to explain the extraordinary affinity of the natural product enterobactin for binding iron.[15] In summary, EFF has been established as a reliable source of valuable information on free and complexed ion carriers, provided careful judgement is exercised in the interpretation of the computer output.

Results and Discussion

Synthesis. The synthesis basically relied on coupling either of the two triscarboxylates, **3** or **4**, with the desired amine, heptylamine **5a**, methylbenzylamine **5b**, or diethylamidoleucine **5c**. The triscarboxylate **3** was prepared from the corresponding tris acid[6] and the triscarboxylate **4** from the corresponding triol by condensation with acrylonitrile, acid-catalyzed hydrolysis, and coupling with pentachlorophenol (Scheme I). All compounds were isolated in good yields after chromatographic purification and fully characterized by their spectroscopic and analytical properties.

Conformation and Ion Binding Properties. Free Ligands. The main structural features of the free ligands were derived from a combination of IR and NMR spectroscopy. All ligands showed rather high IR frequencies of amide–C=O (Table I). This is indicative of nonbonded amide carbonyls. The frequencies of the

Scheme I

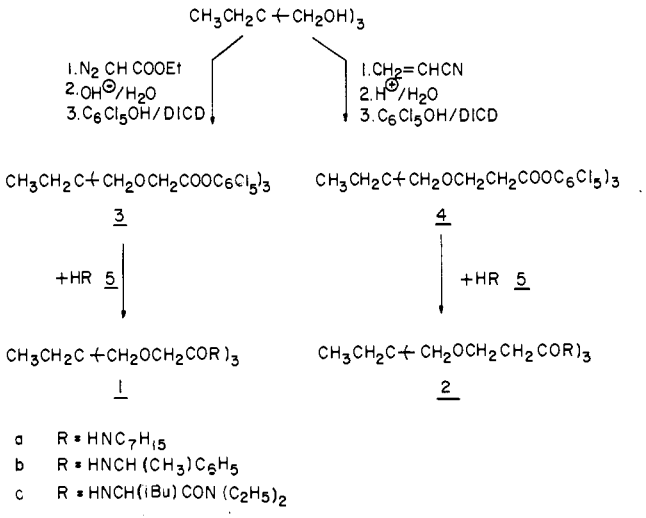

a $R = HNC_7H_{15}$
b $R = HNCH(CH_3)C_6H_5$
c $R = HNCH(iBu)CON(C_2H_5)_2$

C=O[I] groups are systematically lower in chloroform than in acetonitrile, by 2–5 cm^{-1} in type 1 ligands and by 9–12 cm^{-1} in type 2 ligands. The more pronounced solvent effects in type 2 ligands might possibly derive from intrastrand hydrogen bonding between the NH and ether groups in chloroform, which enhances the polarization of the C=O[I] group. In type 1, such H bonding might be less favored as it would lead to a five-membered ring rather than to a six-membered ring. The frequencies of C=O[II] in **1c** and **2c** are much lower than those of C=O[I] but show similar effects.

In the NMR spectra, the diastereotopic methylene protons $C(CH_2OCH_2-$ are magnetically equivalent (Table II), suggesting random orientations of each of the tripodal chains, namely lack of interstrand interactions that would restrict conformational freedom and highlight the asymmetric environment around the diastereotopic protons.

Ca^{2+} Complexes. Experimental Studies. The IR spectra of all the Ca^{2+} complexes in acetonitrile showed a red (bathochromic) shift of the carbonyl stretching frequencies relative to the free ligands. This shift is induced by the ion–dipole interactions and indicates involvement of the carbonyls in binding in all cases (Table I). Some trends in the magnitude of the shifts for the internal

(15) Shanzer, A.; Libman, J.; Lifson, S.; Felder, C. E. *J. Am. Chem. Soc.* **1986**, *108*, 7609–7619.
(16) Lifson, S.; Felder, C. E.; Dobler, M. *Acta. Crystallogr.* **1987**, *B43*, 179–187.

carbonyls (C=O^{I}) in acetonitrile may be discerned, namely the increase from a to b to c and from type 1 to 2. Moreover, in those ligands that contain two types of carbonyl groups, ligands **1c** and **2c**, the induced red shifts of the internal carbonyls were larger than those of the external ones. As elaborated in the Methods, the induced IR shifts provide an estimate of the metal–oxygen distance, as reflected by the elongation of the C=O bond and, consequently, of the strength of the ligand–ion binding. Yet, this correlation is sometimes perturbed by other factors, such as changes in the bond angles,[17] that are likely to also affect the induced shifts.

Using this estimate, one may infer from Table I that the interactions of the carbonyl C=O^{I}, common to all ligands, become stronger as the ligand molecule contains more nonpolar groups. Furthermore, the second carbonyl C=O^{II} seems to bind stronger in **1c** (−19 cm^{-1}) than in **2c** (−8 cm^{-1}).

Solvent dependence of the complexation may be deduced by comparing the IR frequencies in acetonitrile and in chloroform. As is evident from the table, the carbonyl shifts induced upon binding were quite similar in chloroform and in acetonitrile for **1b**, **2b**, and **2c**. This indicates that solvation does not play a major role in the binding process of these ligands. However, pronounced differences were observed for **1c**. The induced shift for the internal carbonyl was significantly smaller in chloroform than in acetonitrile. Similarly, the induced shift for the external carbonyl was zero in chloroform, but significant in acetonitrile.

These observations allow for solvent dependence or even participation in metal binding to **1c** but render solvent participation to the other ligands highly improbable. Moreover, the insignificant solvent dependence for **1b**, **2b**, and **2c** confirms the view that theoretical calculations (vide infra) that treat molecules in vacuo can provide a viable picture of reality.

^{1}H NMR titration (Table II) with calcium perchlorate established a 1:1 ion to ligand stoichiometry in all these ligands. This suggests a hexacoordinated binding of Ca^{2+} to the ligands in types a and b and either hexa- or up to nonacoordination in type c. Single sets of signals were observed in all cases. This indicates either the presence of a single conformation or a mixture of interconverting conformations.

The ^{13}C NMR spectra of the free ligands **1c** and **2c** and of their Ca^{2+} complexes similarly showed single sets of signals (Table III). Most pronounced downfield shifts were observed for the methylene carbons adjacent to the tripodal anchor and the α carbon of the amino acid residue, while upfield shifts occurred for the methylene carbon adjacent to the internal carbonyl, quite in line with the shifts recorded by ^{1}H NMR (vide infra).

Strong downfield ^{13}C NMR shifts were observed for C=O^{I} in both **1c** (+1.450) and **2c** (+2.376). These are in agreement with the corresponding red shifts of C=O^{I} in the IR (−33 and −35 cm^{-1}, respectively) and support the involvement of the C=O^{I} in binding. The C=O^{II} carbonyl shows a very weak downfield shift of the ^{13}C NMR signal in **1c** (+0.222) and none for **2c**, while IR shows a significant red shift (−19 cm^{-1}) in **1c** and a smaller, but not insignificant, one (−8.0 cm^{-1}) in **2c**. The apparent contradiction between the ^{13}C NMR and IR, and the small ^{13}C shift can be attributed to possible shielding of the carbonyl by the isopropyl side chain of the leucyl residue. This explanation is supported by the calculated conformations of **1c** (Figures 9 and 10) that will be discussed in the following text. Studies on valinomycin[18] and on cyclic hexapeptides[19] have shown that metal-ion binding induces chemical shift changes at the carbonyl carbon due to redistribution of the electron density and that more remote carbons may be affected due to conformational changes. In certain cases, changes caused by conformational effects may be opposite to those derived from binding and thereby cause little net change.

Taken together, these data strongly support ion binding to both types of C=O groups in **1c** but predominant (or exclusive) binding to the internal C=O groups in **2c**. This is in agreement with the conclusions drawn from IR data.

In the ^{1}H NMR, ion binding similarly manifests itself by a pronounced downfield shift of all methylene protons of the anchor, as is shown in Table II. The most affected methylenes are those between the ether oxygen and the carbonyl in ligands of type 1, while in ligands of type 2 these are the methylenes between the ether oxygen and the stem carbon that links the three strands. A more interesting feature of Table II is the difference between detailed NMR spectra of the two families of ligands. While only one set of signals was observed for the diastereotopic protons in the Ca^{2+} complexes of chiral type 1 ligands two sets of signals were observed in the complexes of chiral type 2 ligands. (Note: Figure 3 shows the NMR trace of **2b**, both of the free ligand (trace a) and of its Ca^{2+} complex (traces b and c).) The pronounced downfield shift of the α methylene protons is accompanied by a concurrent change of their multiplicity from a singlet (trace a) to a distinguished AB quartet (trace b). Irradiation of the lower field doublet caused a collapse of the higher field counterpart into a singlet (trace c).)

The magnetic equivalence of the diastereotopic protons observed in the calcium complexes of chiral type 1 ligands indicates either the presence of a pseudosymmetric conformation (namely symmetrically affecting the diastereotopic protons) or of an equilibrium mixture of complexes with opposite chiralities. The magnetic nonequivalence observed for the calcium complexes of chiral type 2 ligands, on the other hand, indicates the preponderance of complexes with either right- or left-handed preference. However, the chiral sense of the preferred configuration cannot be deduced from these experimental data and must rest on the calculated conformations (Table IV).

The chirality of the free ligands **1c** and **2c** and their Ca^{2+} complexes was further tested by CD measurements. Similar Cotton effects were observed in free **1c** ($\Delta\epsilon$ = +9.45 at 194 nm) and in its Ca^{2+} complex ($\Delta\epsilon$ = +8.85 at 198 nm). On the other hand, significantly different Cotton effects were observed (see Figure 4) for free **2c** ($\Delta\epsilon$ = +3.15 at 196 nm) and its Ca^{2+} complex ($\Delta\epsilon$ = +12.6 at 210 nm).

These results are indicative of exciton coupling brought about by the alignment of the peptide linkages through ion binding in **2c**–Ca with high chiral preference, but only with small chiral preference for **1c**, in agreement with NMR. The UV and CD spectra of **1b** and **2b** show strong absorptions for the π–π transitions of the phenyl rings, which overshadow the transitions of the amide chromophores. The lack of significant changes of the Cotton effects for the π–π transitions of the phenyl rings when adding Ca^{2+} to either of the ligands indicates either (i) lack of chiral preference of the Ca^{2+} complexes of (ii) coplanar arrangement of the phenyl rings. EFF calculations (see the following text) are compatible with the second alternative.

Taken together, the spectral data represented previously demonstrate pronounced differences in the Ca^{2+}-binding properties of type 1 and type 2 ligands, which are highlighted in the extended ligands **1c** and **2c**. Firstly, type 2 ligands generate chiral Ca^{2+} complexes of pronounced helical preference, while type 1 ligands do not. Secondly, with nine available ion-binding atoms, both **1c** and **2c** may form nonacoordinating complexes, but there are differences between the two that are highlighted by both experiments and calculations. While in **1c** the ether groups may be more weakly bound, in **2c** it is the external C=O^{II} that are weakly bound. Thirdly, ligand **1c** shows pronounced solvent dependence of its ion-binding configuration, while the binding configuration of type 2 ligands including 2c is little solvent dependent.

Type 2 ligands are thus the compounds of choice for the generation of helical structures by exogeneous means. The failure

(17) Lifson, S.; Stern, P. *J. Chem. Phys.* **1982**, *77*, 4542.
(18) Grell, E.; Funck, T.; Sauter, T. *Eur. J. Biochem.* **1973**, *34*, 415.
(19) Deber, C. M.; Madison, V.; Blout, E. R. *Acc. Chem. Res.* **1976**, *9*, 106.
(20) ^{1}H NMR relaxation times provide information on the tightness of the respective calcium complexes. ^{1}H NMR relaxation times were measured on **1d** and **2d** (R = NHCH(*t*-Bu)CONOHCH$_3$) rather than on **1c** and **2c**, since these derivatives show the same spectral features (both IR and NMR) as **1c** and **2c** when binding calcium but exhibit a better resolved NMR spectrum for relaxation time measurements. While the relaxation time for the methylene protons –C(CH$_2$O–) in **1d** dropped to 0.26 s upon binding in ligand **2d**, it dropped to 0.20 s. This indicates more tightness in **2d** than in **1d** and is compatible with shorter Ca–ether oxygen distances in type 2 complex than in type 1 complex.

of type 1 ligands in this respect may be attributed to either the presence of a pseudosymmetric configuration or the presence of equivalent amounts of complexes with opposite chirality. Moreover, the pronounced solvent effects on the ion-binding properties of 1c suggest that the ion-binding cavity may be distorted, so that differences in solvation could affect the energy of alternative ion binding configurations. This would appear not to be the case with the other ligands.

Theoretical Studies. Although relevant information has been obtained on the ion-binding properties of type 1 and type 2 ligands by applying experimental tools, spectroscopic methods suffer from two major limitations: each of the spectroscopic methods provides information on a specific segment of the molecule only and on a superposition of all species present (free and ligated) and their various conformations. Thus, IR allows us to draw conclusions on the involvement of the carbonyl groups in binding, and NMR provides a measure for the proximity of the guest ion to specific atoms (either protons or carbons) and for the extent of anisotropy around specific atoms, while CD measures the interactions between the binding groups and the extent of their chiral preference. It was therefore thought desirable to apply an additional, independent method that would provide a coherent picture of each of the complexes formed and allow us to resolve the equilibrium mixtures into their components. Computer investigations based on the EFF coordinated the various experimental results into a coherent picture and supplemented it with important information not available from spectroscopy. In this respect, EFF served a similar purpose as would X-ray diffraction of single crystals that, unfortunately, could not be obtained.

A thorough conformational scan produced very probably all symmetric low-energy equilibrium states of each complex. For each state, a full set of internal coordinates were obtained, as well as the energy relative to the most stable state. (The crystallographic equivalent would be the structure analysis of all possible isomorphs of each complex.) Table IV represents selected data for all states within 5 kcal/mol of the most stable state of each complex.

The theoretical studies leaned closely on the experimental ones, both in their design and their purpose. In the design, we recognized the fact that all ligands formed 1:1 complexes in acetonitrile; therefore, the ligands of type a and b must be hexacoordinated to Ca^{2+} even when the solvent is ignored, and ligands of type c might yield up to nonacoordination. The structural 3-fold symmetry of all ligands as well as the spectroscopic data were all compatible with the expectation that most complexes are also conformationally C_3-symmetric. We therefore assumed such a symmetry in our scanning and energy minimization algorithms as a matter of computational economy. However, subsequently we waved this assumption. C_3 symmetry was indeed obtained in all cases except one (see the discussion of **1c** in the following text and Table IV).

The main purpose of the EFF calculations was to understand how the structural differences between the a, b, and c types affect the geometric details of their Ca^{2+} complexes and in particular why complexes of type 2, and not of type 1, show chiral preference. The calculations showed that the complexes of type 1 are restricted to more or less prismatic cavities because of the short, single CH_2 link between the ether and carbonyl oxygens. (Prismatic means that the ethers are eclipsed behind the carbonyls if viewed along the symmetry axis of the complex.[21,22] Complexes of type 2, having a longer link $(CH_2)_2$, may adopt more easily an octahedral cavity that is less strained and more suitable to form diastereoisomeric complexes of preferred chirality. The effect of the various R groups on the geometry of the cavity are seen either by comparing the corresponding torsion angles of a, b, and c or by inspection of the stereoviews. Examination of the stereoviews may also give some information about the flexibility of the R groups and the accessibility of the solvent to the Ca^{2+} ion in the cavity.

(21) Wentworth, R. A. D. *Coord. Chem. Rev.* **1972**, *9*, 171.
(22) McMurry, T. J.; Hosseini, M. W.; Garrett, T. M.; Hahn, F. E.; Reyes, Z. E.; Raymond, K. N. *J. Am. Chem. Soc.* **1987**, *109*, 7196.

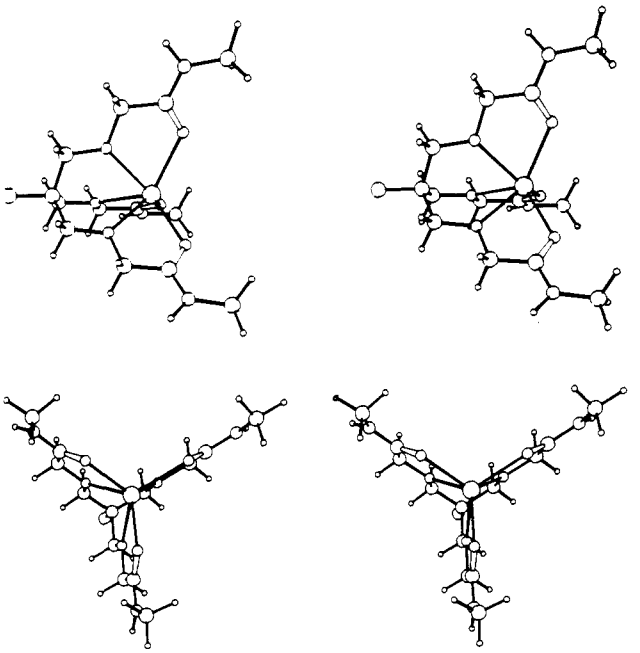

Figure 5. Calculated Ca^{2+} complex of ligand **1a**.

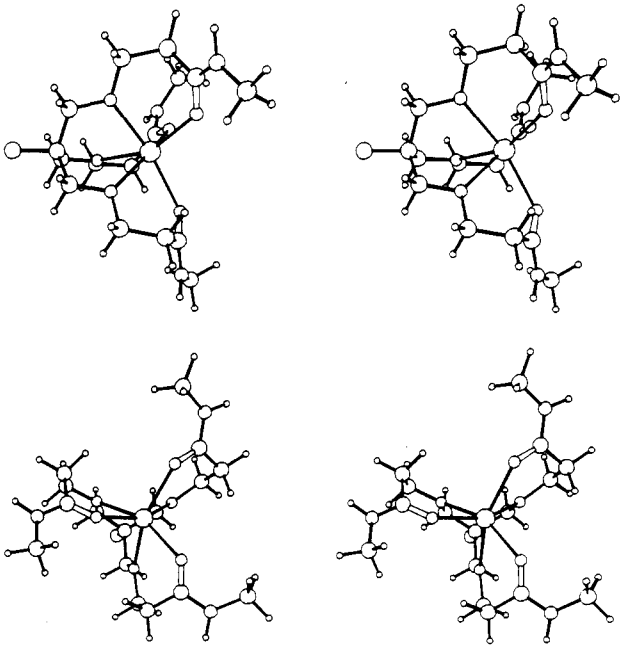

Figure 6. Calculated Ca^{2+} complex of ligand **2a**.

Complexes with R = $-NHC_7H_{15}$ (1a and 2a). Stereoviews of a simplified version of **1a** and **2a** are presented in Figures 5 and 6, respectively, where the *n*-heptyl chain was replaced by a methyl, for the sake of simplicity. The heptyl chain may scan dynamically a very large number of conformations without interfering with the Ca^{2+} binding. This is easily deduced from Figures 5 and 6, where the methyl that substitutes the heptyl is seen to point away from the complex.

The striking feature of the Ca^{2+} complex of **1a** is that its strands are all trans. Its cavity is nonchiral, and essentially prismatic, or more precisely like a truncated pyramid, since the ether oxygens are closer than the carbonyl oxygens to the C_3 symmetry axis. A prismatic cavity is more strained than an octahedral one, but as **1a** cannot make an undistorted octahedral cavity for Ca^{2+}, the calculated nonchiral conformation is the only one available.

The Ca^{2+} complex of **2a** has two distinct conformations that differ in energy by 2.2 kcal/mol, according to our calculations. Both assume octahedral configurations. Since R contains no

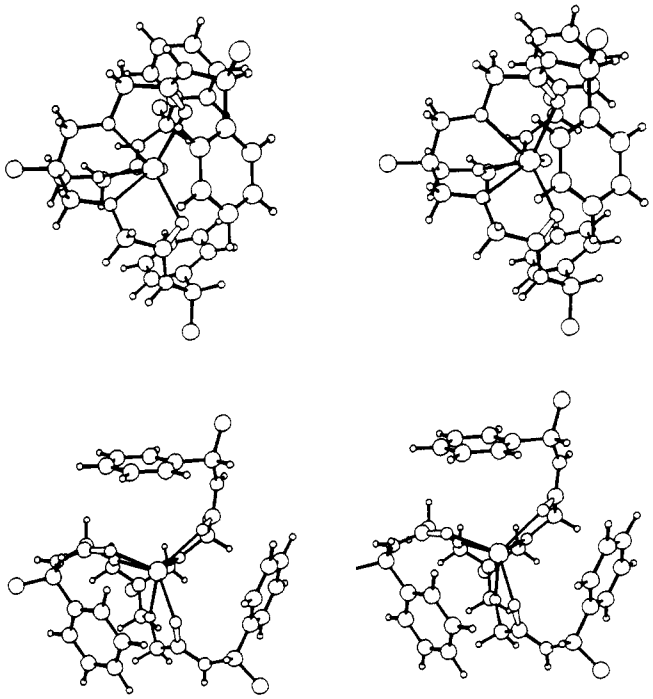

Figure 7. Calculated Ca^{2+} complex of ligand **1b**.

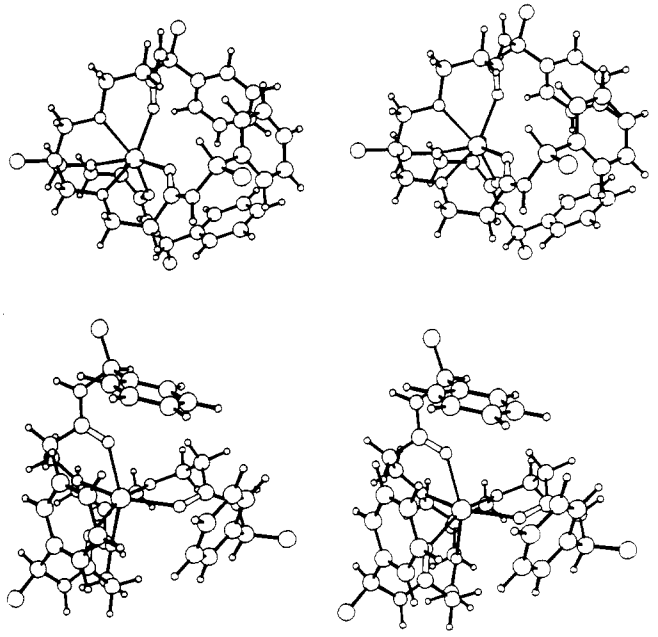

Figure 8. Calculated Ca^{2+} complex of ligand **2b**.

asymmetric center, enantiomeric pairs are formed that have the same energies, and the complexes are racemic.

An examination of Figure 5 shows that the base of the truncated pyramid of the binding cavity of **1a** is perhaps wide enough to accommodate a Ca^{2+}-coordinated acetonitrile solvent molecule. The stereoview of the **2a** complex (Figure 6) shows that the octahedron formed by the six oxygens is not perfect, the carbonyls being rotated along the symmetry axis relative to the ethers by 40° instead of 60°. This complex's cavity seems to be less open to solvation since the carbonyls are closer than those of **1a** to each other and to the Ca^{2+} ion. No experimental evidence is presently available to confirm or reject these suggestions.

Complexes with R = -C*HMeC$_6$H$_5$ (1b and 2b). Figures 7 and 8 show the stereoviews of the most stable complexes of **1b** and **2b** respectively. The methyl group bonded to C* is represented by a single "extended" atom for the sake of simplicity. As is seen in the stereoviews, the simplification is legitimate, since the methyl

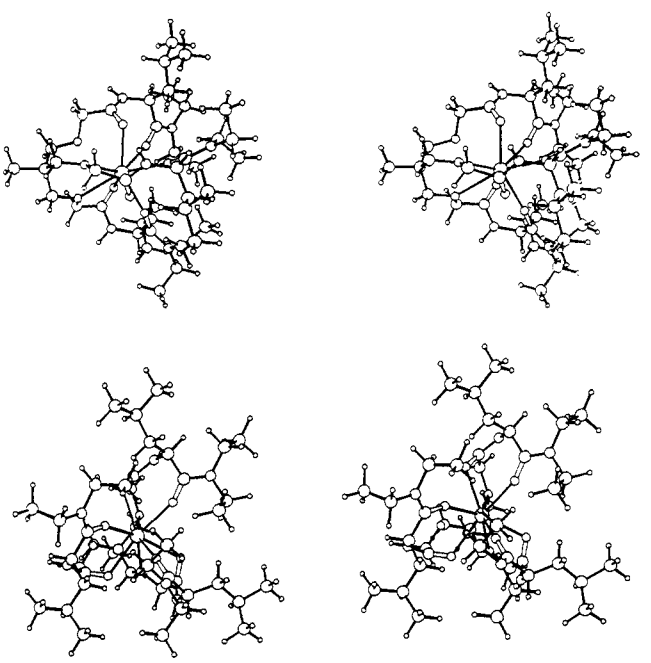

Figure 9. Calculated Ca^{2+} complex 1 of ligand **1c**. Two Ca^{2+}···ether oxygen distances, 2.74 and 2.77 Å, are drawn as bonded, while the longest distance, 2.94 Å, is presented as nonbonded.

points away towards the solvent. The ligand **1b** possesses two different but very similar equilibrium conformations (see Table IV). The prismatic conformation of both is somewhat distorted by the chiral carbon and the bulky phenyl ring that prefer a left-handed twist of the end of the strand. The carbonyls are rotated relative to the ethers by 11° in the most stable conformation and by 3° in the next one. The more stable conformation is shown in Figure 7.

The three conformations of **2b** listed in Table IV are diastereoisomers, due to the chiral carbon on each strand. The most stable conformation, presented in Figure 8, has an approximately Λ configuration, as the carbonyl is rotated relative to the ethers by −39°, and the second conformation is also Λ, with a corresponding rotation of −37°. Only the third, less stable one is Δ. Consequently, the observed configuration of the 2b–Ca^{2+} complex is predicted by the EFF calculations to be predominantly Λ.

These considerations are in accord with the observed NMR signals of the diastereotopic protons in **1b**–Ca^{2+} and **2b**–Ca^{2+} complexes. The signals are split in the **2b** complexes but not in the **1b** complexes. In the **1b** complex, the diastereotopic protons are equivalent, due to the prismatic pseudosymmetry of the complex. Although the protons are not equivalent with respect to the counter-clockwise twist of the ends of the strands with their phenyl rings, these are too far away to have a magnetic effect on the protons. On the other hand, the diastereotopic protons in **2b** show distinct signals due to the predominance of the Λ configuration.

Complexes with Two Carbonyls per Strand. Ligands **1c** and **2c** contain an additional set of ion binding sites, the amido alkyl groups (R = NHC*H-*i*-BuCONEt$_2$). The participation of an additional amide carbonyl in binding was anticipated to strengthen the interactions between the tripodal chains and thereby possibly enhance the chiral preference of the complexes formed. Because of the complexity of these complexes, preliminary calculations were done on analogues that lacked the isopropyl side chains. The calculated structures for **1c** and **2c** were derived from those of the analogues by suitable attachment of the isopropyl side chains. Table IV and Figures 9–11 present the results. The configurations for the coordination of the Ca^{2+} are represented in Table IV as the relative orientation of the first carbonyls relative to the ethers, followed by the relative orientation of the second carbonyls relative to the first carbonyls. The corresponding rotations for the most stable **1c** conformation (average for the three strands) are +43°,

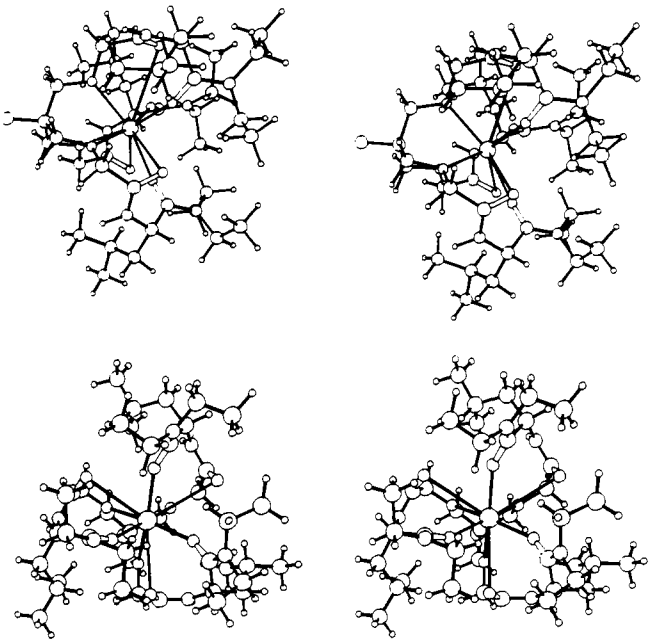

Figure 10. Calculated Ca^{2+} complex 2 of ligand **1c**.

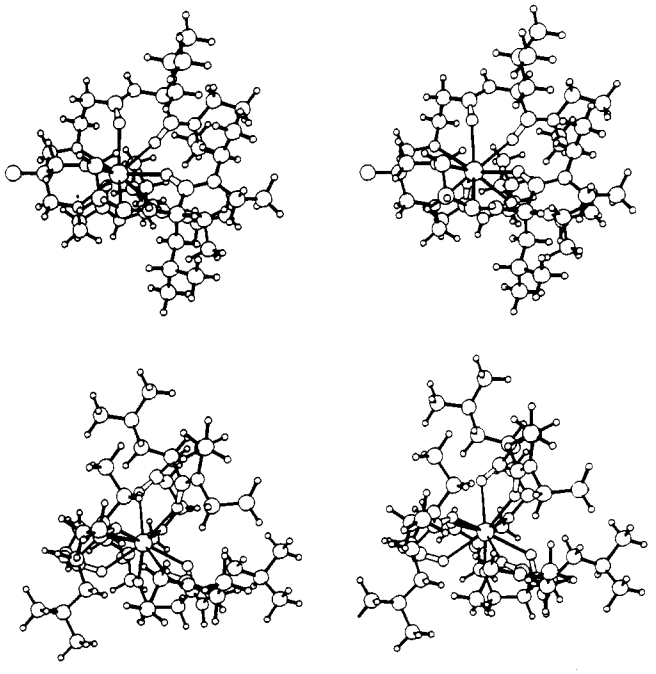

Figure 11. Calculated Ca^{2+} complex of ligand **2c**.

−56°, and for the second conformation, −1°, +60°. The corresponding rotations for **2c** are +59°, −45°.

Our initial results for **1c**, constrained to C_3 symmetry, were found to be at variance with the experimental NMR and IR data. The latter suggested that Ca^{2+} binds more tightly to the internal carbonyls (close to the anchor) than to the external ones. In contrast to these observations, the EFF indicated stronger binding to the external carbonyls. In appreciation of the comments of one of the reviewers, it occurred to us that steric hindrance between the side chains (one isopropyl and two *N*-ethyl groups per strand) and the binding ligands may destabilize the C_3-symmetric conformation in favor of a nonsymmetric one. Thereupon all available conformations of both **1c** and **2c** were reminimized with the C_3 constraint removed. An independently conformational scan of **1c** free from symmetry constrains was also made.

The result was that all conformations of **2c** and all but one of **1c** retained the C_3 symmetry. Only the most stable **1c** conformation lost its symmetry. The fact that **1c**, due to steric hindrance, was found to deviate from C_3 symmetry while the slightly larger **2c** retained it is a very interesting result. For, as can be seen in Figure 9 and Table IV, the **1c** binding cavity is more distorted than that of **2c**. This is consistent with the strong solvent dependence observed in **1c** and not in **2c**. If a given structure can form a binding cavity with an optimal size and geometry for a given metal, it can easily compete against any solvent medium. If, on the other hand, the cavity is badly distorted, some solvent interactions may be strong relative to the molecular ligating interactions, while others may be weak, leading to a pronounced solvent dependence on binding. Thus, the predicted **1c** carbonyl–Ca^{2+} distances represent complexation in vacuum or crystal phase better than in acetonitrile, and are certainly not applicable to chloroform.

Concluding Remarks

We have previously shown that interlocking the chains of C_3-symmetric trispeptides through a network of interchain H-bonds generates conformationally constrained structures of preferred chiral sense.[1] Interlinking the chains of tripodal molecules by exogeneous means, i.e., binding Ca^{2+} ions, was anticipated to similarly create organized structures of defined helicity even in polar solvents where H-bonds are weak or altogether broken. The realization of the idea was sought with two types of ligands, type 1 and type 2, that are suited to form five-membered and six-membered chelate rings, respectively. When binding Ca^{2+}, these ligands were found to form a large variety of complexes, including hexa- or nonacoordinated ones. These complexes may be of either prismatic or octahedral geometry. While prismatic geometry is characterized by reflection symmetry and therefore is inherently unfit to form chiral complexes, octahedral geometry lacks reflection symmetry and is therefore amenable for the generation of chiral complexes. Type 1 ligands have been found to form either prismatic or distorted Ca^{2+} complexes, due to the strain imposed by the ligands' stem. On the other hand, type 2 ligands, which have more conformational degrees of freedom to adjust themselves, form octahedral-type complexes. Because of the presence of asymmetric centers, the right- and left-handed isomers of these complexes are diastereomeric. Therefore, one of them becomes energetically favored, resulting in the generation of chiral Ca^{2+} complexes of preferred handedness. Extension of the type 2 ligands by adding more binding cavities is envisioned to provide binders that accommodate two metal ions in a defined chiral sense such as to create helical complexes. The chiral ligands described above also bind Li^+ ions and Mg^{2+} ions, although with different coordination numbers than those observed with Ca^{2+} ions. The selectivity of these ligands and their potential as neutral ionophores are under current investigation.

Experimental Section

Synthesis of Ca^{2+}-Ion Binders. General Methods. Melting points are determined on a Fisher-Johns apparatus and are uncorrected. They are given in degrees Celsius. Infrared spectra measured with a Perkin-Elmer 681 grating spectrometer, with a Fourier-transform IR Nicolet Mx-1 spectrometer, or with Fourier-transform IR Cignus 25 Mattson spectrometer and are given in per centimeter (cm^{-1}) units. Proton NMR spectra are measured on Varian FT-80a or Bruker WH 270 NMR spectrometers. All chemical shifts are reported in δ units downfield from TMS as internal standard, and the J values are given in hertz. Splitting patterns are designated as follows: s, singlet; d, doublet; t, triplet; m, multiplet; q, quartet.

Thin-layer chromatography (TLC) is performed on aluminum sheets precoated with silica gel (Merck, Kieselgel 60 F 254, Art. 5549) or with alumina (Riedel-De Haen). Column chromatography separations are performed on silica gel (Merck 70–230 mesh ASTM) or on neutral alumina, Activity I. Flash column chromatography separation are performed on silica gel (Merck 230–400 mesh ASTM).

THF is dried by treating overnight with KOH and subsequent filtration through basic alumina. Chloroform, dichloromethane, and acetonitrile are dried by filtration through basic alumina.

Preparation of $EtC(CH_2OCH_2COOC_6Cl_5)_3$ (3). A total of 2 g (6.50 mmol) of triacid, 6.382 g (24 mmol) of pentachlorophenol, and 255 mg (2.08 mmol) of 4-(dimethylamino)pyridine are dissolved in 120 mL of dry acetonitrile and treated at 0 °C with 3.75 mL (24 mmol) of diisopropylcarbodiimide. The reaction is stirred for 4 days at room temper-

ature. Then, acetonitrile is removed and the crude mixture chromatographed on silica gel (CCl_4/EtoAc (80:20)) to give 1.789 g of **3** (yield 25%). NMR ($CDCl_3$): δ 4.47 (s, CH_2CO, 6 H); 3.64 (s, CH_2O, 6 H), 0.94 (t, CH_3, J = 7, 3 H). IR ($CDCl_3$): 1802 (CO) cm^{-1}.

Preparation of EtC($CH_2OCH_2CH_2COOC_6Cl_5$)$_3$ (4). A 13.4-g portion of triol (0.1 mol) is treated dropwise with 1.0 mL of 40% aqueous NaOH, and then 22 mL (0.33 mol) of acrylonitrile (freshly purified by passing through neutral alumina) is added such that the temperature does not exceed 30 °C. Then, the mixture is stirred over night at room temperature, neutralized with diluted aqueous HCl, dissolved in 500 mL of ethyl acetate, washed with water, dried, and concentrated to give 25.45 g of trinitrile. The crude product is hydrolyzed by treating 2.93 g with 3.6 mL of concentrated HCl in an oil bath of 95–100 °C for 4 h. After being cooled to room temperature, the residue is suspended in ethyl acetate, washed with water, dried, and concentrated to give 2.49 g of triacid. A total of 4.9 g of crude triacid are dissolved in 500 mL of acetonitrile (dried over alumina), 13.2 g of pentachlorophenol and 610 mg of 4-(dimethylamino)pyridine are added, and the mixture is cooled in an ice bath and treated with 7.5 mL of diisopropylcarbodiimide. Then, the mixture is allowed to warm to room temperature and stirred for 1–2 days. Concentration in vacuo and chromatography on silica gel (CCl_4/EtOAc (98:2, 95:5)) provides 2.5 g of the triscarboxylate (mp 146–150 °C). NMR ($CDCl_3$): δ 3.80 (t, $-OCH_2C$, 3.35 (s, CCH_2O, 6 H), 2.91 (t, CH_2CO, 6 H). IR ($CDCl_3$): 1825 (CO) cm^{-1}.

Preparation of EtC($CH_2OCH_2CONHC_7H_{15}$)$_3$ (1a). A 0.452-g (0.429-mmol) portion of triphenolate **3** is dissolved in 20 mL of dry CH_2Cl_2. Then, 0.255 mL (1.716 mmol) of *n*-heptylamine and 25 mg (0.214 mmol) of *N*-hydroxysuccinimide are added, and the reaction mixture is stirred at room temperature for 2 days. The solvent is evaporated and the crude mixture rapidly chromatographed on neutral alumina ($CHCl_3$/MeOH(95:5)) to give 0.231 g of **1a** (yield 90%). Mp: 65–67 °C.

Preparation of EtC($CH_2OCH_2CONHCHCH_3C_6H_5$)$_3$ (1b). A 0.650-g (0.616-mmol) portion of triphenolate **3** is dissolved in 13 mL of dry CH_2Cl_2. Then, 0.318 mL (2.467 mmol) of *S*-(α)-methylbenzylamine and 35.5 mg of *N*-hydroxysuccinimide are added, and the reaction mixture is stirred for 2 days. The solvent is evaporated and the crude mixture chromatographed, first rapidly on neutral alumina ($CHCl_3$/MeOH-(95:5)) to remove pentachlorophenol then on silica gel (120 mL of $CHCl_3$/MeOH(95:2), and then on $CHCl_3$/MeOH(95:5)) to give 0.292 g of **1b** as an oil (yield 85%).

Preparation of NH_2CH-*i*-BuCONEt$_2$ (5c). A 5.442-g (26-mmol) portion of *N*,*N*-dicyclohexylcarbodiimide and 100 mg of (dimethylamino)pyridine are added at 0 °C to a solution of 6.355 g (24 mmol) of *Z*-L-leucine and 2.759 g (24 mmol) of *N*-hydroxysuccinimide in 100 mL of dry THF. The reaction mixture is allowed to stand in the refrigerator overnight. The formed dicyclohexylurea is filtered and washed with dry THF. To the combined filtrate and washings is added 2.491 mL (24 mmol) of diethylamine dissolved in dry THF and the reaction mixture stirred at room temperature for 5 days. Then, THF is removed and the crude mixture chromatographed on neutral alumina ($CHCl_3$ and then $CHCl_3$/MeOH(98:2)) to give 3.376 g of protected amide as an oil (yield 43%). NMR ($CDCl_3$): δ 7.33 (m, ArH, 5 H), 5.50 (b s, NH, 1 H), 5.09 (s, $ArCH_2$, 2 H), 4.60 (m, NHCHCO, 1 H), 3.40 (m, NCH_2, 4 H), 1.79–1.41 (m, CH_2CH, 3 H), 1.24–0.88 (several triplets, CH_3, 12 H). IR ($CDCl_3$): 1716 (CH_2OCON), 1644 (CON) cm^{-1}. A solution of 2 g (6.25 mmol) of protected amide *Z*-NHCH*i*-BuCONEt$_2$ in EtOH is added to 0.5 g of Pd/C (5%) in 50 mL – of EtOH and the mixture hydrogenated under atmospheric pressure for 45 min. The mixture is filtered and evaporated to dryness to provide 0.986 g of the desired product of **5a** as an oil (yield 62%). NMR ($CDCl_3$): δ 3.50 (m, NHCHCO, 1 H), 3.30 (m, NCH_2, 4 H), 1.46–1.24 (m, CH_2CH_3 3 H), 1.20–0.90 ppm (several signals, CH_3, 12 H). IR ($CDCl_3$): 1632 (CON) cm^{-1}.

Preparation of EtC(CH_2OCH_2CONH-*i*-BuCONEt$_2$)$_3$ (1c). A 0.433-g (0.411-mmol) portion of triphenolate **3** is dissolved in 40 mL of dry CH_2Cl_2. Then 0.305 g (1.644 mmol) of NH_2CH-*i*-BuCONEt$_2$ and 23 mg of *N*-hydroxysuccinimide are added to the solution, and the reaction mixture was stirred for 3 days. The solvent is evaporated and the crude mixture chromatographed rapidly on neutral alumina ($CHCl_3$) and then flash-chromatographed on silica gel (500 cm^3 of $CHCl_3$, 400 cm^3 of $CHCl_3$/MeOH(99:1), 300 cm^3 of $CHCl_3$/MeOH(98:2), and 300 cm^{-3} of $CHCl_3$/MeOH(95:5)) to give 0.187 g of **1c** as an oil (yield 56%).

Preparation of EtC($CH_2OCH_2CH_2CONHC_7H_{15}$)$_3$ (2a). By use of the same procedure as for EtC($CH_2OCH_2CONHC_7H_{15}$)$_3$, the derivative EtC($CH_2OCH_2CH_2CONHC_7H_{15}$)$_3$ is prepared (using dry $CHCl_3$ as solvent), purified by chromatography on neutral alumina, and eluted with 200 mL of $CHCl_3$, 500 mL of $CHCl_3$/MeOH(98:2), and $CHCl_3$/MeOH(95:5) to give the desired product **2a** in 77% yield. Mp: 63–67 °C.

Preparation of EtC($CH_2OCH_2CH_2CONHCHCH_3C_6H_5$)$_3$ (2b). By use of the same procedure as for EtC($CH_2OCH_2CONHCHCH_3C_6H_5$)$_3$, the derivative EtC($CH_2OCH_2CH_2CONHCHCH_3C_6H_5$)$_3$ is prepared (using dry $CHCl_3$ as solvent, purified by chromatography on neutral alumina, and eluted with $CHCl_3$/MeOH(95:5) to give the desired product **2b** as an oil in 92% yield.

Preparation of EtC($CH_2OCH_2CH_2CONHCH$-*i*-BuCONEt$_2$)$_3$ (2c). By use of the same procedure as for EtC($CH_2OCH_2CONHCH$-*i*-BuCONEt$_2$)$_3$, the derivative EtC($CH_2OCH_2CH_2CONHCH$-*i*-BuCONEt$_2$)$_3$ is prepared (using dry $CHCl_3$ as solvent), purified by chromatography on neutral alumina, and eluted with 400 mL of $CHCl_3$/MeOH(98:2) and 700 mL of $CHCl_3$/MeOH(95:5) to give the expected product **2c** as an oil in 70% yield.

Titration Experiments. Titrations were performed by adding to 10 mM (or 20 mM) solutions of the ligands in CD_3CN (or in $CDCl_3$) aliquots of stock solutions of $Ca(ClO_4)_2$ in CD_3CN and measuring the NMR and IR spectra.

EFF Calculations. The calculations were done on Weizmann Institute's central IBM 3090 computer, according to the algorithm described in refs 10 and 12. The atom charge on the ether oxygen was taken as the same as carbonyl O, –0.46, with appropriate countercharges on the adjacent methylenes. The Lennard-Jones parameters derived for K^+ were used for Ca^{2+}, together with a charge of +2.00, after checking that these yielded ion–oxygen binding distances consistent with values obtained from a scan of the Cambridge Database[23] (~2.4 Å). The conformations were constrained to C_3-rotational symmetry during most of the energy minimizations, except for the final calculations of **1c** and **2c**.

A special conformational scanner developed in our laboratory for tripod ion-binding structures was used to find all conformations of **1a** and **2a** binding Ca^{2+} within 5 kcal/mol of the energy minimum. For convenience, the extended alkyl sidechains were replaced by extended methyl atoms. The low-energy conformations for **1b** and **2b** were derived from the above by attaching and scanning over all conformations of the appropriate $-CHMeC_6H_5$ side chains. The conformational scanning of **1c** and **2c** was done in stages. First, the nonchiral side chains R = $-C^*H_2CONMe_2$ were attached to **1a** and **2a**. Later, chiral isobutyl sidechains were attached to C*, and the NMe end groups were replaced by *N*-ethyl ones. Finally, the C_3 constraint was removed. An independent, nonsymmetric conformational scan of the full **1c** yielded no additional stable conformations. The stereoviews were prepared by use of ORTEP.

Acknowledgment. We thank Dr. H. Gottlieb from University Bar-Ilan for determining the ^1H NMR relaxation times, Mr. M. Ben-Avner for technical assistance in the NMR measurements, and the United States–Israel Binational Science Foundation for support of this work.

Registry No. 1a, 132080-14-9; **1b**, 132080-15-0; **1c**, 132080-16-1; **2a**, 132080-17-2; **2b**, 132080-18-3; **2c**, 132080-20-7; **3**, 132080-19-4; **4**, 110374-69-1; **5c**, 63618-45-1; $CH_3CH_2C(CH_2OCH_2COOH)_3$, 38945-32-3; $CH_3CH_2C(CH_2OCH_2CN)_3$, 53067-27-9; $H_2NC_7H_5$, 111-68-2; (*S*)-PhCH(NH_2)CH_3, 2627-86-3; Z-Leu-OH, 2018-66-8; $NHEt_2$, 109-89-7; Ca^{2+}, 14127-61-8.

(23) Allen, F. H.; Bellard, S.; Brice, M. D.; Cartwright, B. A.; Doubleday, A.; Higgs, H.; Hummelink, T.; Hummelink-Peters, B. G.; Kennard, O.; Motherwell, W. D. S.; Rodgers, J. R.; Watson, D. G. *Acta. Crystallogr.* **1979**, *B35*, 2331.